



OPEN ACCESS

EDITED BY

Mohammad Hojjat-Farsangi,
Karolinska Institutet (KI), Sweden

REVIEWED BY

Nooran Elleboudy,
Ain Shams University, Egypt
Angela Rita Elia,
Institute of Oncology Research (IOR),
Switzerland

*CORRESPONDENCE

Jing-Yuan Fang
jingyuanfang@sjtu.edu.cn
Huimin Chen
huimin.chan@foxmail.com

SPECIALTY SECTION

This article was submitted to
Cancer Immunity
and Immunotherapy,
a section of the journal
Frontiers in Immunology

RECEIVED 13 August 2022

ACCEPTED 03 October 2022

PUBLISHED 20 October 2022

CITATION

Xie Y, Chen H and Fang J-Y (2022)
Amino acid metabolism-based
molecular classification of colon
adenocarcinoma *via in silico* analysis.
Front. Immunol. 13:1018334.
doi: 10.3389/fimmu.2022.1018334

COPYRIGHT

© 2022 Xie, Chen and Fang. This is an
open-access article distributed under
the terms of the [Creative Commons
Attribution License \(CC BY\)](#). The use,
distribution or reproduction in other
forums is permitted, provided the
original author(s) and the copyright
owner(s) are credited and that the
original publication in this journal is
cited, in accordance with accepted
academic practice. No use,
distribution or reproduction is
permitted which does not comply with
these terms.

Amino acid metabolism-based molecular classification of colon adenocarcinoma *via in silico* analysis

Yile Xie, Huimin Chen* and Jing-Yuan Fang*

State Key Laboratory for Oncogenes and Related Genes, Key Laboratory of Gastroenterology and Hepatology, Ministry of Health, NHC Key Laboratory of Digestive Diseases, Division of Gastroenterology and Hepatology, Shanghai Institute of Digestive Disease, Renji Hospital, School of Medicine, Shanghai Jiao Tong University, Shanghai, China

Amino acid metabolism is closely related to the occurrence and development of colon adenocarcinoma (COAD). Studies on the relationship between COAD and the expression of amino acid metabolism are still rare. Based on *in silico* analysis, we used 358 amino acid metabolism-related genes (AAMRGs) to determine the amino acid metabolism characteristics and then classified COAD into two distinct subtypes, namely AA1 and AA2. Then we analyzed the clinical characteristics, somatic mutation landscape, transcriptome profile, metabolism signatures, immune infiltration, and therapy sensitivity of these two subtypes. The AA1 subtype had inferior overall survival and was characterized by lower amino acid metabolic activity, higher tumor mutation burden, and higher immune cell infiltration, while AA2 displayed higher metabolic activity and relatively better survival. Furthermore, the AA1 subtype was likely to benefit from irinotecan in chemotherapy and immune checkpoint blockade therapy including programmed cell death protein-1 (PD-1) and cytotoxic T-lymphocyte-associated protein-4 (CTLA-4) immune checkpoint inhibitor but was resistant to targeted therapy cetuximab. The AA2 subtype showed higher sensitivity to 5-fluorouracil and oxaliplatin. To provide perspectives on cell-specific metabolism for further investigation, we explored metabolic activity in different cell types including lymphocytes, mast cells, myeloid cells stromal cells, and epithelial cells *via* colorectal cancer single-cell data. Additionally, to assist in clinical decision-making and prognosis prediction, a 60-AAMRG-based classifier was generated and validated in an independent cohort.

KEYWORDS

amino acid metabolism, colon adenocarcinoma, classification, prognosis, immune signature, therapy

Introduction

Colorectal cancer is the third most common new case of cancer and the second most common cause of cancer death in 2020 (1). Colon adenocarcinoma (COAD) accounts for 69.7% of all colorectal cancer (2). Due to the high heterogeneity, COAD brings more challenges to clinical treatment and management. The heterogeneity derives from many aspects, including genetic and epigenetic alterations, tumor microenvironment (TME) cell population diversity, microbiome multiformity, and metabolism adaptations. The treatment methods for COAD are mainly surgery, chemotherapy, targeted therapy, and immunotherapy and the therapeutic response is also influenced by diverse factors. Therefore, it is necessary to have a deeper understanding of the biodiversity of COAD, especially its relationship with clinical characteristics. For instance, the previous classical gene expression-based classification consensus molecular subtypes (CMSs) captured the intrinsic heterogeneity of colorectal cancer, in which colorectal cancer could be classified into 4 distinguishing types, CMS1 (immunotype), CMS2 (classical type), CMS3 (metabolic type), and CMS4 (mesenchymal type) (3). In addition, some research on COAD molecular typing and prediction models based on transcriptome data have emerged, which provide new aspects for accurate classification and treatment effect prediction of COAD (4, 5).

Metabolic reprogramming is a major feature of tumors and is involved in rapid growth, evasion of immune clearance, and adaptation to the metastatic environment (6). There has been some thorough and detailed research focused on the role of glucose metabolism, lipid metabolism, and amino acid metabolism in cancers (6, 7). Amino acid metabolism has extremely extensive effects in producing materials for metabolite biosynthesis, epigenetic modification, bioenergy supply, detoxifying ammonia, and maintaining intracellular redox status (8). Emerging studies have pointed out the significant participatory role of specific amino acid metabolisms, such as glutamine (9, 10), tryptophan (11), cystine (12), and serine (13), in COAD progression and resistance to various therapies. Amino acid-related metabolic genes may serve as a prognostic prediction model for COAD. In addition, targeting amino acid metabolism may reshape the immune microenvironment, overcome immunotherapy resistance, and improve the efficacy of existing treatments (7). A growing number of metabolism-related molecular models have been applied to COAD classification (14–16); however, the amino acid metabolism-related gene expression-based classifier has not been reported.

Recognizing that the high-throughput transcriptomics mirrors numerous molecular features behind tumor phenotype and clinical behavior, we envisioned that classifying COAD tumors based on amino acid metabolism will deepen our understanding of the metabolic heterogeneity of COAD from a new perspective and contribute to precise therapy. In this

study, we aim to divide primary COAD samples into subgroups based on curated amino acid metabolism-related genes (AAMRGs), and evaluate the clinical variables, molecular features, potential therapy response through *in silico* bioinformatic analysis, then establish a classifier assisting clinical decision-making and prognosis prediction.

Materials and methods

Patient and sample data collection

COAD transcriptome data for classification were accessed from The Cancer Genome Atlas (TCGA), and 420 primary COAD patients with transcriptome data with corresponding overall survival information extracted from the Genomic Data Commons (GDC) Data Portal (<https://portal.gdc.cancer.gov/>) were enrolled in this study for *in silico* analysis. Patients with an overall survival time of fewer than 30 days were removed to prevent bias. The gene expression value was transformed into \log_2 [transcripts per kilobase million (TPM) + 1] for further analysis. Missing values in clinical information were excluded when comparing differences in clinical characteristics between subtypes. Gene somatic mutation data (MAF files) were available in 372 of the above 420 patients in TCGA-COAD datasets and were also obtained *via* the GDC Data Portal.

Colon adenocarcinoma subtypes based on amino acid-related genes

For further *in silico* analysis, a total of 360 amino acid metabolism-related genes (AAMRGs) were acquired from previous work (Table S1) (17, 18), and 358 of them were detected in TCGA-COAD transcriptome data. Then, we performed K-means consensus clustering with the gene expression profiles of 358 AAMRGs to identify subtypes by using the CancerSubtypes package in R software (19). The following details were set for subtyping: number of repetitions = 1,000 bootstraps; $pItem = 0.8$ (resampling 80% of any sample); $maxK=10$ (k-means clustering with up to 10 clusters). An appropriate number of clusters was determined based on the clustering results and clinical ease of use. The Kaplan–Meier method with a log-rank test was performed to compare overall survival differences between the subtypes.

Characteristics specific to the AA subtypes

To investigate multiple characteristics between AA subtypes, we compared clinical and molecular features between the two AA subtypes. A Chi-square test was used to explore the clinical

feature distribution between different AA subtypes. The somatic mutation profile of COAD patients from TCGA was analyzed with the maftools R package (20). Gene expression profiles were also utilized for calculating the distance of samples from four CMSs *via* the CMScaller R package (21). Transcriptomic alterations were compared between AA subtypes with differentially expressed gene analysis *via* the limma R package (22)(Table S2). Pathway enrichment analysis of gene ontology biological progress (GOBP) was performed based on differentially expressed genes (P value <0.05 and log₂FC >0.5), and gene set enrichment analysis (GSEA) based on the Reactome pathway database was carried out with genes with statistical significance *via* cluster profile (23) and the ReactomePA R package (24).

To evaluate different biological process activities based on gene expression profiles, single-sample gene set enrichment analysis (ssGSEA) was performed to compute enrichment scores *via* the GSVA R package (25), and 114 metabolism-related pathways (26) and 5 immune-related signatures, including anti-CTLA-4 resistance-associated MAGE-A (CRMA) (27), IFN-gamma response (28), immune checkpoint (29), hot tumor (30) and EGFR signatures (31), were collected for ssGSEA. Pearson correlation analysis was applied to investigate the correlation between amino acid metabolism-related genes and immune-related signature enrichment scores.

Estimation of immune cell infiltration

The CIBERSORT algorithm was used to estimate the infiltration of a total of 22 immune cell populations in COAD samples by using their cell-specific gene signatures (32). Additionally, the Microenvironment Cell Populations-counter (MCP-counter) method was performed to evaluate the abundance of eight immune and two nonimmune stromal cell populations *via* the MCPcounter R package (33), and the ESTIMATE algorithm was applied for estimating immune and stromal fractions *via* the estimate R package (34).

Generation and validation of the AA classifier

The top 30 significantly differentially expressed AAMRGs with the largest log₂FC value in both AA subtypes were selected for the development of the prediction model, and thus, a 60-gene classifier was generated (Table S3). For validation, the 60-gene classifier was carried out on the TCGA-COAD dataset itself and an independent dataset GSE41258 from the Gene Expression Omnibus (GEO, <http://www.ncbi.nlm.nih.gov/geo/>) database based on the Nearest Template Prediction (NTP) classification, a method that allows us to apply given signatures to individual

sample class prediction on GenePattern (<https://www.genepattern.org/>). Overall survival analyses were also performed by Kaplan–Meier methods and compared by the log-rank test. The concordance correlation coefficient between the AA subtypes and predicted AA subtypes in the TCGA cohort was calculated *via* the DescTools R package (35).

Estimation of the potential therapy response

To predict the response to three first-line treatment drugs (5-fluorouracil, oxaliplatin, and irinotecan) between the two AA subtypes, the oncoPredict R package (36) was implemented using ridge regression to estimate the half-maximal inhibitory concentration (IC₅₀) for each COAD sample based on the gene expression profile from the Genomics of Drug Sensitivity in Cancer 2.0 (GDSC2) database (37). All parameters were set to recommended values.

To predict target therapy (cetuximab and bevacizumab) and immunotherapy (CTLA4 and PD1 monoclonal antibody) response between AA subtypes, SubMap analysis on GenePattern was applied for comparing the expression data between AA subsets with colorectal cancer patients treated with cetuximab (GSE5851) or bevacizumab (GSE53127) and melanoma patients treated with immunotherapies extracted from previous work (38).

Estimation of cell type-specific metabolic activities based on single-cell data

Colorectal single-cell RNA sequence datasets GSE144735 were downloaded from the GEO database. The VISION algorithm was used to score each cell type in metabolic pathways obtained from KEGG and REACTOME *via* the scMetabolism R package (39).

Statistical analyses

Analyses were performed based on R program (V.4.1.1). Overall survival analyses were performed by Kaplan–Meier methods and compared by the log-rank test. A Chi-square test was carried out to compare clinical characteristics, gene mutation rates, and therapy response ratios between AA subtypes. Pearson correlation analysis was applied to investigate the correlation between amino acid metabolism-related genes and immune-related signature enrichment scores. The Wilcoxon test was used to compare the means of the two groups. P value < 0.05 was considered statistically significant.

Results

Consensus clustering identifies two metabolism subtypes in COAD

Based on 358 detected genes of 360 previously reported amino acid metabolism-related genes (17, 18) (Table S1), we carried out K-means consensus clustering on transcriptome data comprising 420 primary COAD patient samples from TCGA and divided them into two subtypes, AA1, and AA2. The overall survival of these two subtypes was significantly differentiated, and the AA1 subtype displayed a worse prognosis (Figures 1A–C). For further exploration, we investigated the clinicopathological features of these two subtypes. There were no significant differences in age, gender, or American Joint

Committee on Cancer (AJCC) stage between the two subtypes (Figures 1D, E). We observed that the AA1 phenotype could be described as a COAD subtype predominantly originating from the right colon and was associated with a higher MutL Homolog 1 (MLH1) silent mutation rate, a higher proportion of microsatellite instability (MSI) status, and a CpG island methylator phenotype (CIMP) subtype compared to the AA2 subtype (Figures 1F–I). Univariate analysis demonstrated that the AA subtype was an independent predictor for clinical prognosis (Figure 1J). Furthermore, using CMS classification (3), samples of the AA1 subtype were mainly classified into CMS1 and CMS4, the worst prognosis subtype in CMSs, while samples of AA2 were mainly classified into CMS2 and CMS3 with relatively better survival (Figures 1K, L). These results

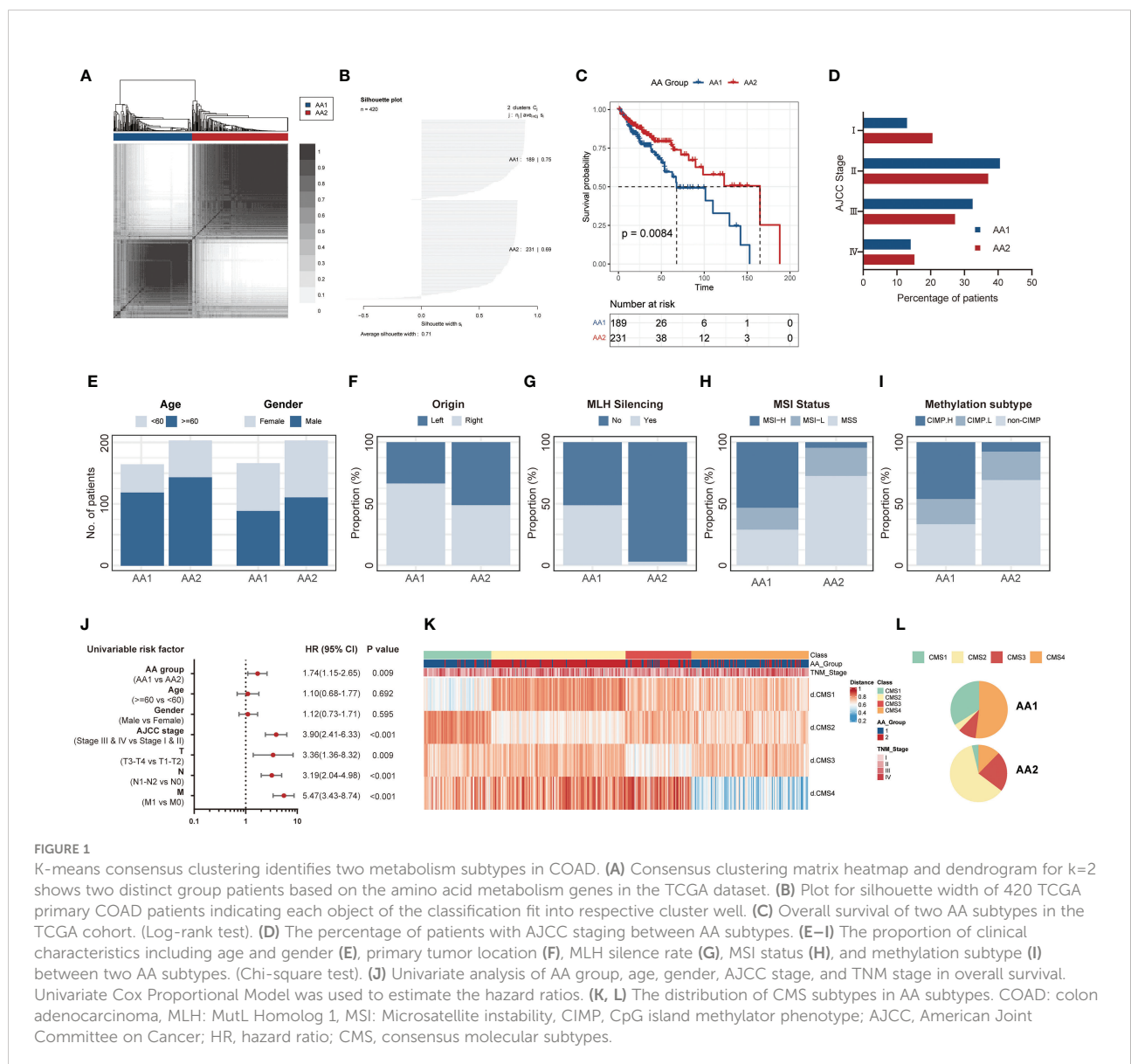


FIGURE 1

K-means consensus clustering identifies two metabolism subtypes in COAD. (A) Consensus clustering matrix heatmap and dendrogram for k=2 shows two distinct group patients based on the amino acid metabolism genes in the TCGA dataset. (B) Plot for silhouette width of 420 TCGA primary COAD patients indicating each object of the classification fit into respective cluster well. (C) Overall survival of two AA subtypes in the TCGA cohort. (Log-rank test). (D) The percentage of patients with AJCC staging between AA subtypes. (E–I) The proportion of clinical characteristics including age and gender (E), primary tumor location (F), MLH silencing rate (G), MSI status (H), and methylation subtype (I) between two AA subtypes. (Chi-square test). (J) Univariate analysis of AA group, age, gender, AJCC stage, and TNM stage in overall survival. Univariate Cox Proportional Model was used to estimate the hazard ratios. (K, L) The distribution of CMS subtypes in AA subtypes. COAD: colon adenocarcinoma, MLH: MutL Homolog 1, MSI: Microsatellite instability, CIMP, CpG island methylator phenotype; AJCC, American Joint Committee on Cancer; HR, hazard ratio; CMS, consensus molecular subtypes.

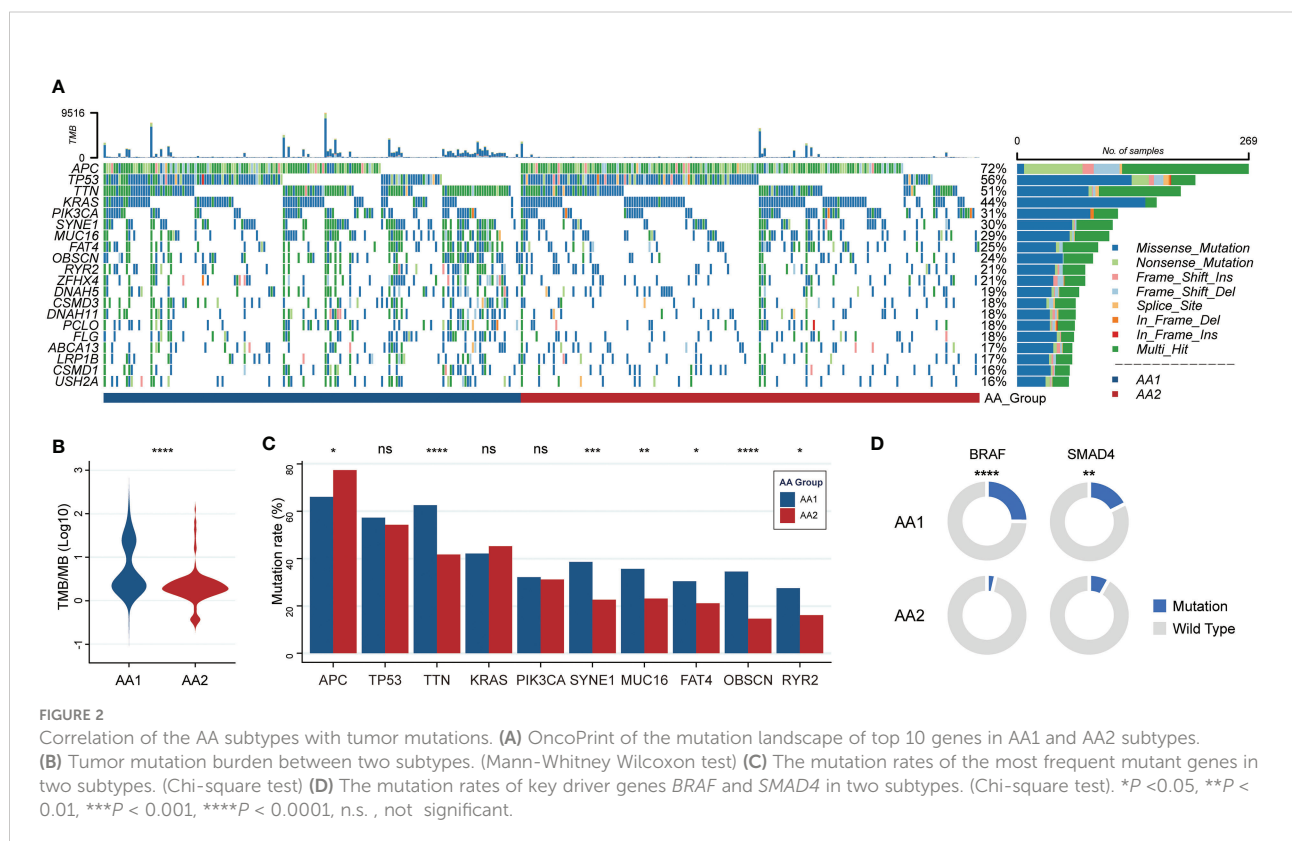
suggest that the heterogeneity in amino acid metabolism may be connected with the prognosis of COAD.

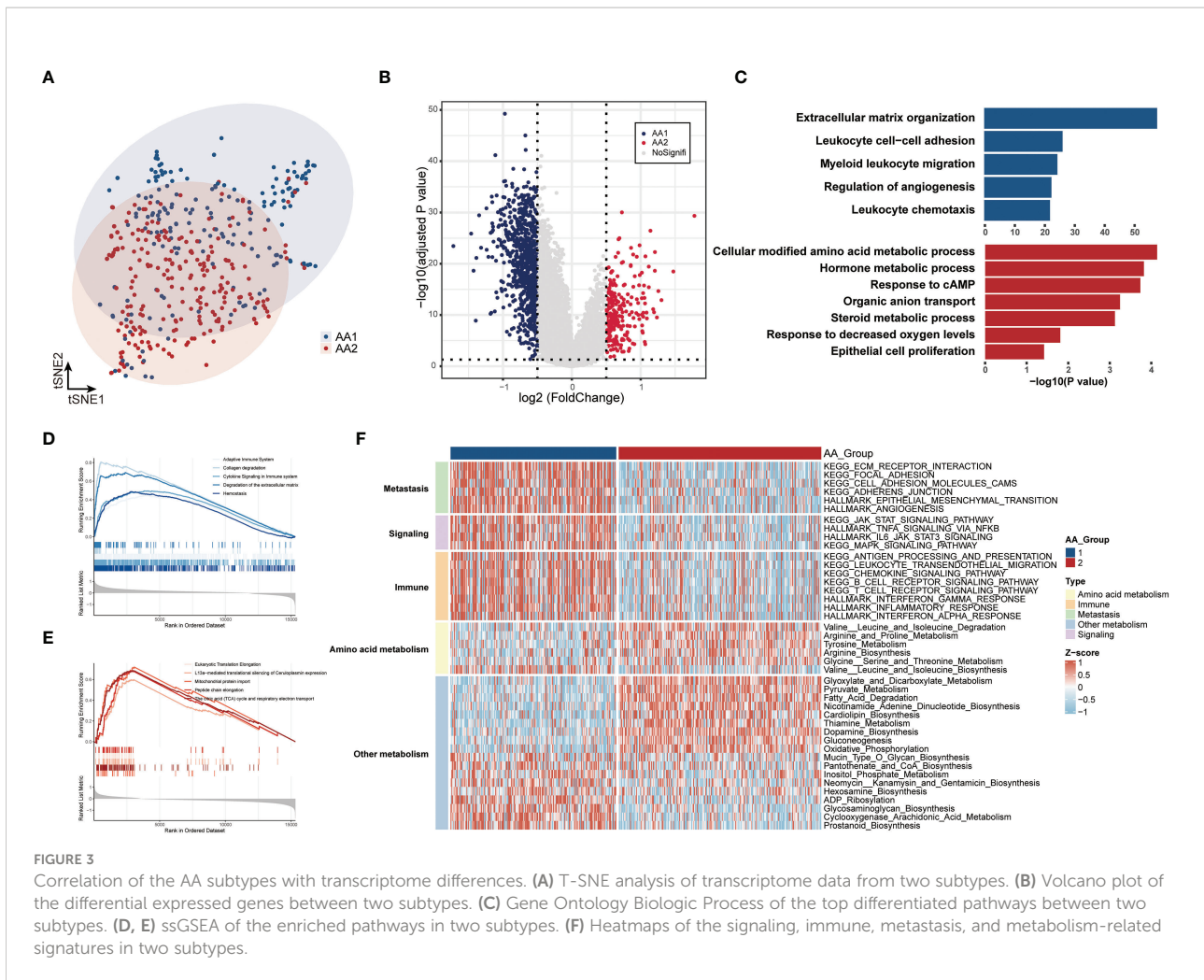
Correlation of the AA subtypes with tumor mutations

The fact that AA1 tumors were intensively associated with hypermutation status and highly consistent with hypermutated CMS1 subtypes drove us to investigate whether there were mutation landscape differences between the two subtypes. The somatic mutation panorama showed that the overall mutation rate in AA1 was higher (Figure 2A). Consistent with the clue offered by MSI status and CMS classification, the tumor mutation burden (TMB) was significantly higher in the AA1 subtype than in the AA2 subtype (Figure 2B). *APC*, *TP53*, *TTN*, *KRAS*, *PIK3CA*, *SYNE1*, *MUC16*, *FAT4*, *OBSCN*, and *RYR2* were the top 10 mutant genes in two subgroups, among which *TTN*, *SYNE1*, *MUC16*, *OBSCN*, and *FAT4* acquired higher mutation rates in the AA1 subtype while *APC* acquired higher mutation rates in AA2 subtype (Figure 2C). In addition to those high-frequency mutations, we examined the mutation rates of several driver genes reported previously (40), *BRAF* (41), *SMAD4* (42), and *EGFR* (43, 44), and found that AA1 displayed higher *BRAF* and *SMAD4* mutation rates (Figure 2D).

Correlation of the AA subtypes with transcriptome differences

To better characterize the features of the two subtypes, we performed transcriptomic data differential analysis. The gene expression pattern differed significantly between AA1 and AA2 (Figures 3A, B) (Table S2). Pathway enrichment analysis based on gene ontology biological process (GOBP) showed that AA1 enriched pathways were mainly focused on ‘extracellular matrix organization’, ‘immune cell chemotaxis and migration’, and ‘adaptive immune’, while AA2 enriched pathways in energy metabolism such as ‘amino acid, hormone, steroid metabolic process’, and ‘cell proliferation’ (Figure 3C). Gene set enrichment analysis (GSEA) based on the Reactome pathway database drew a similar conclusion: AA1 was enriched with extracellular matrix remodeling and immune pathways, while AA2 was closely related to metabolism-related events. Furthermore, we analyzed the activation status of pathways involved in various biological processes, including signaling, immunity, metastasis, and metabolism, between the two subtypes through ssGSEA (Figure 3F). The AA1 subtype was also active in several colon cancer progression-related signaling, immunity, and metastasis pathways such as epithelial-mesenchymal transition, angiogenesis, JAK-STAT signaling, and inflammatory pathways (Figure 3F). In amino acid metabolism,





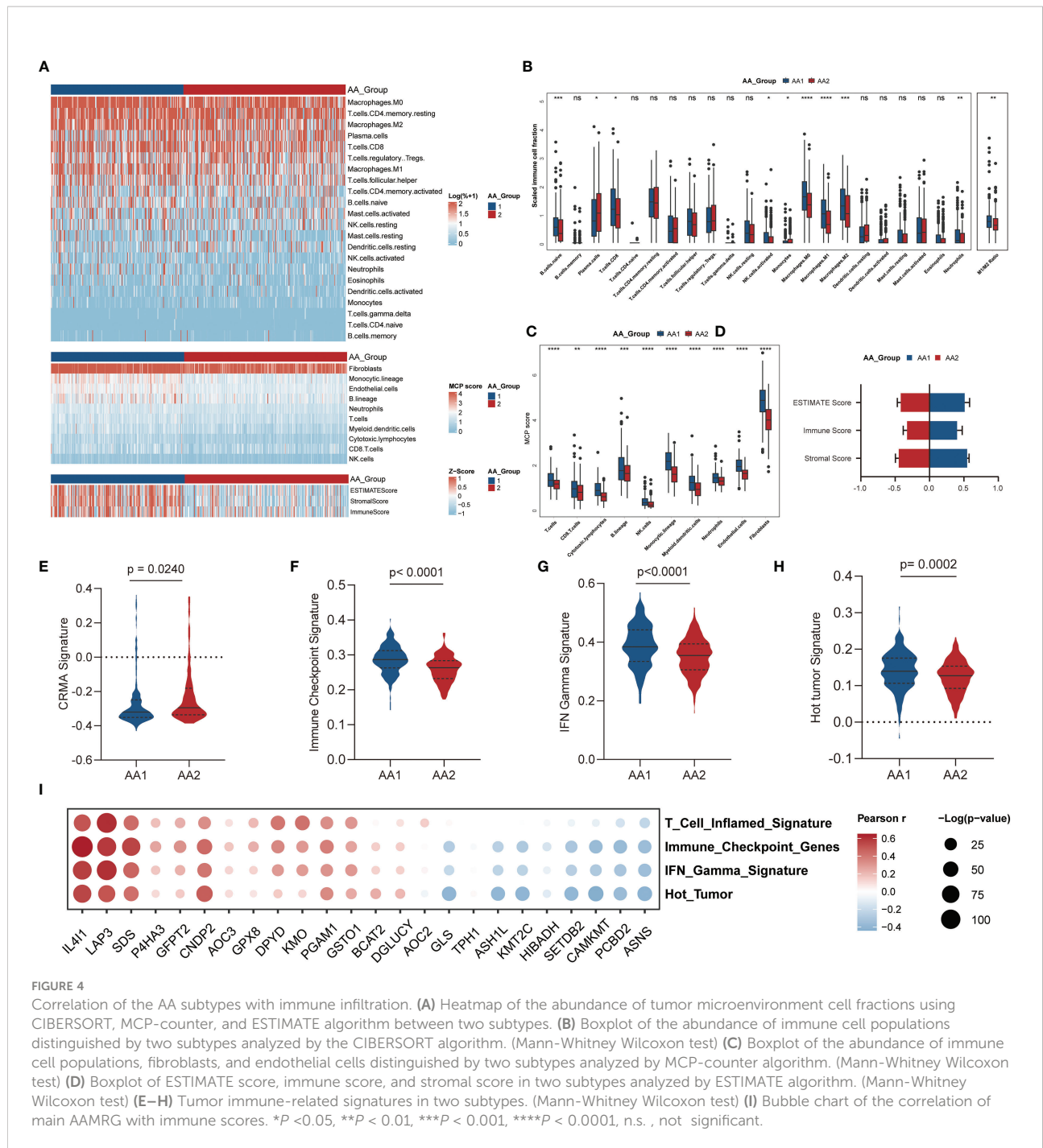
AA1 was only activated in ‘valine, leucine and isoleucine biosynthesis pathway’, while AA2 had an extensive activation in ‘arginine and proline metabolism’, ‘tyrosine metabolism’, ‘glycine, serine and threonine metabolism’ pathways. In addition, among other metabolism pathways, we found several inflammatory pathways, including ‘ADP ribosylation’, ‘glycosaminoglycan biosynthesis’, ‘prostanoid biosynthesis’, and ‘cyclooxygenase arachidonic acid metabolism’, were significantly activated in AA1. While energy metabolism-related pathways such as ‘oxidative phosphorylation’, ‘gluconeogenesis’, and ‘fatty acid degradation’ were highly activated (Figure 3F).

Correlation of the AA subtypes with immune infiltration

The evolution of cancer is strongly dependent on the complicated tumor microenvironment (TME), which comprises a variety of cell types, including fibroblasts, endothelial cells, and immune cells. Given the distinct differences in immune pathway

characteristics in the two subtypes (Figures 3C–F), we investigated the immune microenvironment features through three algorithms: CIBERSORT (32), Microenvironment Cell Populations-counter (MCP-counter) (33), and ESTIMATE (34) (Figure 4A). Via the CIBERSORT algorithm, 22 immune cell fractions were calculated in each sample, and the fractions of naive B cells, CD8 T cells, activated NK cells, monocytes, macrophages (M0, M1, M2), and neutrophils were significantly higher in the AA1 subtype, while plasma cells were higher in the AA2 subtype (Figure 4B). Notably, the M1/M2 macrophage ratio was higher in AA1 (Figure 4B). The MCP-counter results showed that all evaluated types of immune cells and mesenchymal cells (endothelial cells and fibroblasts) were significantly enriched in AA1 than in AA2 (Figure 4C). The immune score and stromal score of the ESTIMATE algorithm resembled the conclusions of the previous two algorithms (Figure 4D).

We observed that the CRMA score was higher in the AA2 subtype (Figure 4E), which suggested that the AA2 subclass may be linked with primary resistance to anti-CTLA-4 therapy. Other immune-related signatures, such as IFN gamma (28), immune



checkpoint (29), and hot tumor (30) were higher in AA1 (Figures 4F-H), which indicated that AA1 may benefit more from immunotherapy. Correlation analysis of immune-related signatures with differential amino acid metabolism-related genes showed that *IL4I1*, *LAP3*, and *SDS* were the top three genes with the highest positive correlation, while *ASNS*, *PCBD2*, and *CAMKMT* were negatively correlated with immune signatures (Figure 4I).

Correlation of the AA subtypes with treatment prognosis

According to the aforementioned widely differed molecular characteristics between the AA1 and AA2 subtypes, we hypothesized that the two subtypes might also benefit differently from chemotherapy, immunotherapy, or targeted therapy. We predicted the half maximal inhibitory

concentration (IC50) of three first-line chemotherapy drugs of patients in the AA1 and AA2 subtypes based on the GDSC2 database and found that AA2 was more sensitive to 5-fluorouracil and oxaliplatin, while AA1 was more sensitive to irinotecan (Figure 5A), which helped us to provide a rational drug application for AA subtypes. In addition, we found that AA1 was more sensitive to Janus Kinase (JAK) inhibitor JAK_8517 and AZ960_1250, insulin-like Growth Factor I Receptor (IGF1R) inhibitor IGF1R_3801, and Heat Shock Protein 90 inhibitor Luminespib_1559 (which could effectively down-regulate IGF-1R β protein). AA2 was sensitive to TGF β /SMAD4 receptor inhibitor SB505124 (Figure 5B). Moreover, using the SubMap algorithm, we also explored the correlation between the AA subtypes and response groups toward the targeted drugs cetuximab and bevacizumab. There was little significance between the AA subtypes and the bevacizumab response group, but AA1 was more relevant to the cetuximab nonresponse group (Figure 5B), which was consistent with the lower EGFR score in the AA1 subtype (Figure 5C). Then, we compared the expression profiling of AA1 and AA2 with the melanoma dataset containing 47 patients

who received a programmed cell death protein-1 (PD-1) immune checkpoint inhibitor or cytotoxic T-lymphocyte-associated protein-4 (CTLA-4) immune checkpoint inhibitor (38). AA1 exhibited a significant association with the CTLA4- and PD1-sensitive groups, which indicated that the AA1 subtype was more likely to benefit from immune checkpoint blockade therapy (Figure 5D).

Generation and validation of the AA classifier in the GEO dataset

For better clinical application, we generated a classifier with a total of 60 genes containing the top 30 AAMRGs in each AA subtype (Table S3). The concordance with the original prediction based on Consensus Cluster was evaluated in the TCGA cohort. We observed a concordance of 88.8% in the AA1 subtype and 89.1% in the AA2 subtype, which indicated that the 60-gene signature can reproducibly determine the COAD-AA classification. Besides, the concordance correlation coefficient (CCC) between the AA subtypes and the predicted AA subtypes

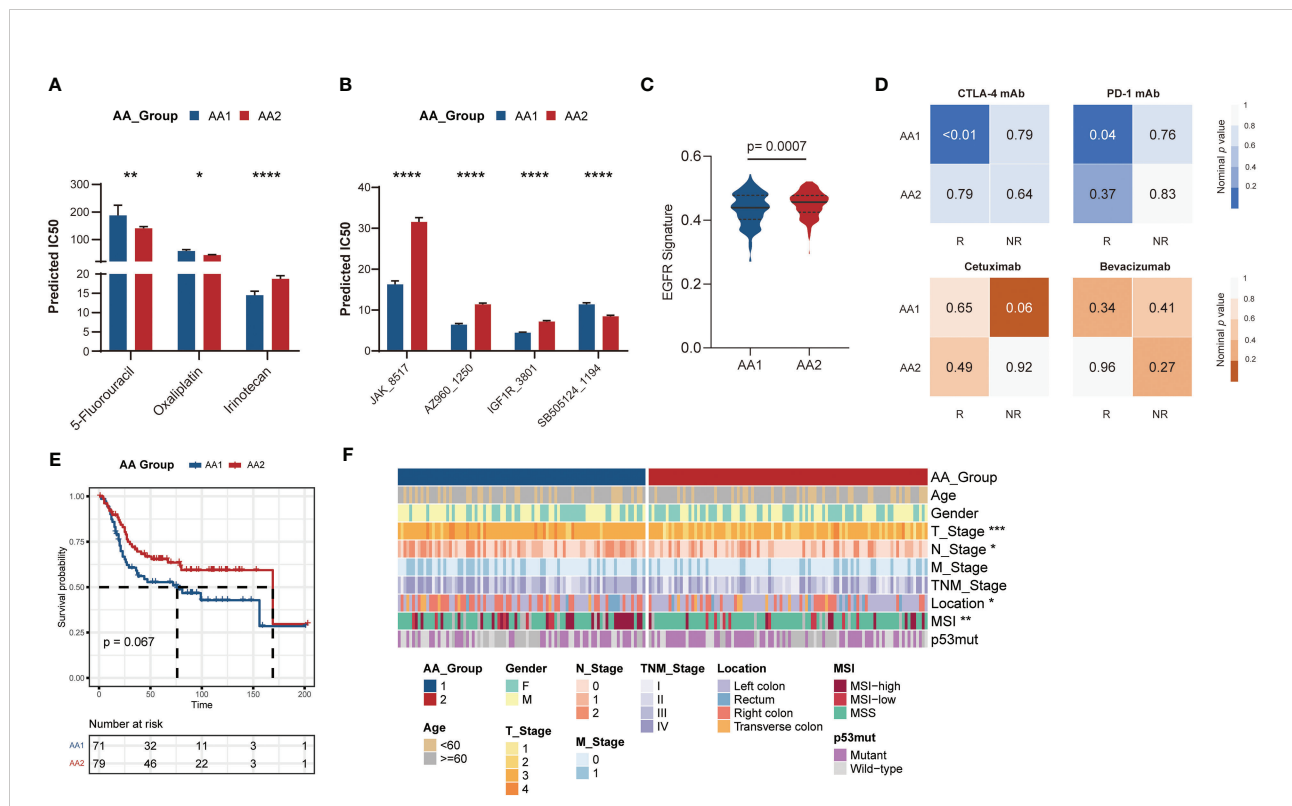


FIGURE 5 Correlation of the AA subtypes with treatment prognosis. Generation and validation of the AA classifier in the GEO dataset. **(A)** Bar chart of the predicted IC50 of COAD chemotherapy drugs 5-fluorouracil, oxaliplatin, and irinotecan of two AA subtypes. (Mann-Whitney Wilcoxon test). **(B)** Bar chart of the predicted IC50 of JAK inhibitor (JAK_8517 and AZ960_1250), IGF1R inhibitor (IGF1R_3801), and TGF β /SMAD4 receptor inhibitor (SB505124_1194) of two AA subtypes. (Mann-Whitney Wilcoxon test) **(C)** EGFR signatures in two subtypes. (Mann-Whitney Wilcoxon test) **(D)** SubMap analysis for immunotherapy prediction in melanoma cohort (upper) and the response of targeted therapy cetuximab and bevacizumab in colorectal cancer cohort (bottom). **(E)** Overall survival of two AA subtypes typed by 60-gene classifier in GSE41258 cohort. (Log-rank test) **(F)** Clinical and pathological characteristics of the two subtypes in the GSE41258 cohort. * $P < 0.05$, ** $P < 0.01$, *** $P < 0.001$, **** $P < 0.0001$.

was 0.78 (95% CI, 0.74-0.81). Subsequently, we validated the classifier in an independent colorectal cancer dataset, GSE41258, through the NTP algorithm. Similarly, the AA1 subclass in the GSE41258 dataset had poorer overall survival (Figure 5E), a higher proportion of MSI, right colon location, and worse T and N stages (Figure 5F).

Exploration of the cell type-specific metabolic activity landscape with single-cell data

To further comprehend the metabolic status among different cell types in the tumor environment, we calculated the cell type-specific KEGG and REACTOME metabolic pathway activity in a single-cell RNA sequence dataset (39). As marked with underlines in the figure, we found that amino acid-related metabolic pathways, including branched-chain amino acids (BCAAs) (valine, leucine, and isoleucine), tryptophan, glutathione, and arginine metabolism, were almost highly activated in epithelial and stromal cells (Figures 6A, B). Among immune cells, mast cells and myeloid cells acquired relatively higher amino acid metabolisms activity, such as glutamate and glutamine, arginine, and histidine metabolism. However, lymphocytes, including T cells and B cells, displayed a relatively lower metabolic level. In addition to amino acid metabolism, other metabolic processes differed in the AA subtypes like glycosaminoglycan biosynthesis and arachidonic acid metabolism, highly upregulated in the AA1 subtypes, were mainly found to be active in both stromal cells and mast cells.

Discussion

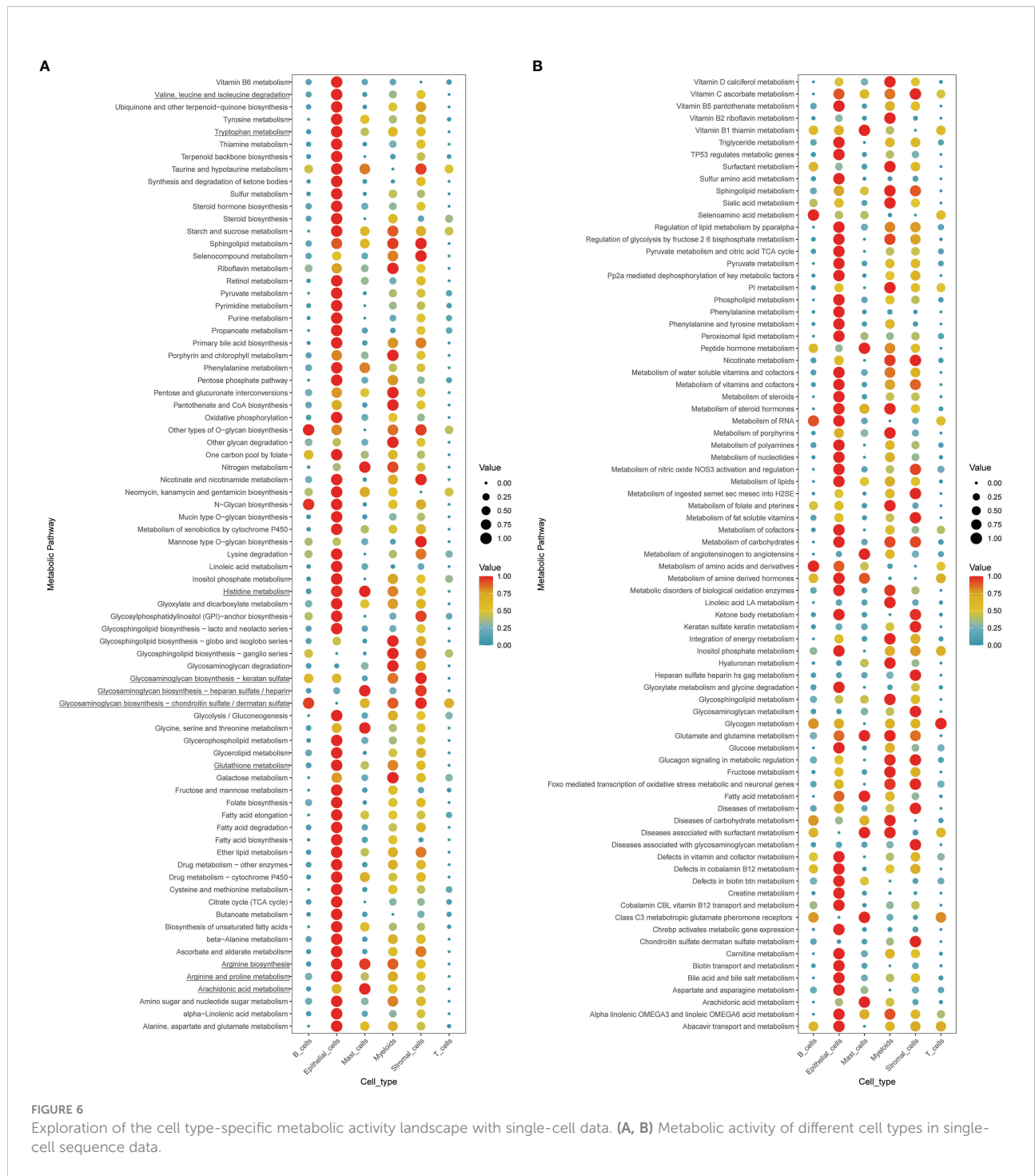
In this study, for the first time, we established an amino acid metabolism-related gene expression-based classification to predict prognosis and assist individual treatment decisions in COAD. The two AA subtypes displayed distinct overall survival and clinical and molecular features. AA1 had an inferior overall survival and harbored 'inactive amino acid metabolism' and 'inflammatory and mesenchymal TME' characteristics. The higher MSI, TMB, and inflammatory microenvironment of AA1 contribute to its sensitivity to ICB therapy. AA2 was associated with 'active amino acid metabolism' features, and a higher EGFR score predicted that AA2 could benefit from EGFR inhibitor treatment.

Primary tumor location is associated with distinct differences in the microbiome, clinical characteristics, chromosomal and molecular characteristics, treatment, and prognosis (45). Left colon cancer has a better prognosis than right colon cancer under routine chemotherapy and targeted treatment. The primary locations of AA1 subtype tumors are mostly in the right colon. The right COAD is characterized by

MSI, CIMP status, and BRAF/PI3KCA mutation (45) consistent with AA1 features. Meanwhile, AA1 harbors more BRAF mutations. The right COAD has been thought to arise through an alternative serrated neoplasia pathway (46). A sessile serrated adenoma is highlighted by BRAF^{V600E} point mutation, CIMP, and MLH1 methylation compared to classic adenomas (47). These results suggest that the amino acid metabolic features of right COAD and sessile serrated adenoma might be more biased toward AA1.

Next, we explored the characteristics of these two subtypes from mutation, transcriptome, tumor environment, and therapeutic response aspects. Mutations in oncogenes or tumor suppressors are known to alter cellular metabolism to fuel cancer (48). At the DNA level, there was a higher tumor mutation burden in AA1. BRAF and SMAD4 are highly mutated in the AA1 subtype, and SMAD4 mutation correlates with worse clinical outcomes and resistance to chemotherapy (49). In addition, we found high-frequency mutations, such as TTN (muscle protein), SYNE1 (structural proteins), MUC16 (O-glycosylated protein), OBSCN (cytoskeletal proteins), and FAT4 (maintaining cell polarity), all of which were higher in the AA1 than AA2 type. TTN, SYNE1, and MUC16 mutations are associated with increased TMB and correlated with an enhanced response to ICB immunotherapy in solid tumors (50–53). OBSCN mutation might promote tumor proliferation, migration, and metastasis (54, 55). FAT4 mutation could predict survival outcomes for stratifying patients with colorectal cancer independent of TNM staging (56). These high-frequency mutations deserve further study to explore their biological functions in COAD.

Amino acids play many important roles in cell growth and survival, including participating in the TCA cycle, nucleobase synthesis, and regulating redox balance (57). Our results showed that AA2 had an extensive activation in 'arginine and proline metabolism', 'tyrosine metabolism', 'glycine, serine, and threonine metabolism' pathways. Arginine can be endogenously synthesized or taken up from the environment, and is critically involved in processes including the synthesis of nitric oxide and polyamines to maintain rapid proliferation (58). Due to the low expression of arginine synthesis-related enzyme, arginine auxotrophic tumors cannot endogenously synthesize sufficiently, and thus tend to depend on the uptake of extracellular arginine. Pegzilarginase, an inducer of arginine deprivation may promote an immunostimulatory TME and improve the immunotherapy effect (59). Besides, a variety of catabolic enzymes involved in polyamine catabolism are potential targets for the treatment of COAD (58). Metabolites, rate-limiting enzymes, and ARH in tryptophan metabolism are related to CRC. Upregulated tryptophan catabolites such as kynurenine block effector T cell activation and trigger T cell apoptosis to prevent the immune system from successfully destroying cancer cells. Specifically, the enzyme IDO1 breakdown tryptophan into kynurenine may be a potential therapeutic target for colorectal cancer (57). Serine and glycine



contribute carbon to the serine, glycine, one-carbon (SGOC) metabolic network, which plays a role in various cellular processes, including nucleotide synthesis, lipid, and protein synthesis, methylation metabolism, polyamine metabolism, and redox balance. Serine and glycine were also reported as immunosuppressive metabolites and promoted the survival of non-transformed TME cells to form a protective niche for tumors.

Hence, limiting serine metabolism may have substantial therapeutic implications for immunotherapy (60). In our results, the activation of these three metabolic sectors in AA2 is consistent with this non-beneficiary feature of immunotherapy. Therefore, we wonder whether the combination of specific metabolic inhibitors and immunotherapy can improve the response rate. Branched-chain amino acid (BCAA) metabolism, containing

valine, leucine, and isoleucine, is the only upregulated amino acid metabolic pathway in the AA1 subtypes. Emerging studies have shown that the BCAA metabolic enzymes BCAT1 and BCAT2 are aberrantly activated and functionally required for malignant tumors such as chronic myeloid leukemia (61), acute myeloid leukemia (62), and PDAC (63). High levels of BCAT1 also displayed a DNA hypermethylation phenotype (62). In addition, tumor cell BCAAs and their metabolites, such as branched-chain α -keto acid, can maintain the proliferative status of Treg cells (64) or reduce the phagocytic activity of macrophages (65). BCAT1 can also downregulate glycolysis in T cells (66). Together, BCAA metabolic reprogramming plays a significant role in immune suppression, thus boosting cancer progression (67). However, clinical and biological research on BCAAs and COAD is still rare. Our work indicated that the combination of BCAA starvation or metabolic enzyme inhibitors with conventional tumor therapy might further improve the prognosis of the AA1 subtype, which needs more evidence to prove the mechanism.

Although these two subtypes did not differ significantly in age, gender, TNM stage, or AJCC stage, their prognosis was significantly different. Considering the tumor microenvironment, we hypothesized that the differences in stromal and immune-related factors contribute to the prognosis. By comparing the transcriptome data, we found that immune-, ECM- and metastasis-related pathways were significantly enriched in the AA1 subtype. ADP ribosylation, glycosaminoglycan biosynthesis, prostanoid biosynthesis, and cyclooxygenase arachidonic acid metabolism were upregulated in AA1. ADP-ribosylation (ADPR) is a posttranslational modification (68); however, its relationship with COAD survival is unknown. Glycosaminoglycan is a component of the ECM that plays an important role in supporting cells and providing a platform for cell interactions (69). Dysregulation of glycosaminoglycan metabolism, which is highly upregulated in AA1 and mainly expressed by stromal cells and mast cells, promotes sustained proliferation, angiogenesis, metastasis, and evasion of the immune response (69). PGE has been shown to promote tumor progression by silencing tumor suppressors, inducing cancer stem cell formation, enhancing immunosuppressive cells, and impairing cytotoxic CD8 T-cell and NK-cell functions (70). These dysregulated pathways in AA1 indicated that the enriched and activated stromal cells may largely contribute to the inferior prognosis of AA1. The heterogeneity of AA subtypes might also determine the different sensitivities of therapies. AA1 was more sensitive to irinotecan, ICB therapy (both anti-CTLA-4 and anti-PD-1), and bevacizumab. Meanwhile, AA1 harbored more resistance to cetuximab. Referring to the BRAF mutate COAD, the combination of anti-BRAF, anti-MEK, and anti-EGFR targeted therapy may improve the efficacy in AA1. In contrast, AA2 was more sensitive to 5-fluorouracil and oxaliplatin and may benefit more from cetuximab treatment. Finally, we established a 60-AAMRG-based classifier to simulate the 358-AAMRG classifier well, which is more concise and convenient in clinical application.

In conclusion, we built a new binary classifier of COAD, and using the AAMRG classifier can partially explain the heterogeneity of COAD. This classifier would help to timely select AA1 subtype patients who would benefit more from precise therapy and achieve better clinical outcomes.

Data availability statement

The original contributions presented in the study are included in the article/[Supplementary Material](#). Further inquiries can be directed to the corresponding authors.

Author contributions

YX were responsible for the analysis, interpretation of data, graphing and manuscript draft. HC and J-YF supervised the whole analysis and provided guidance and instructions. All authors contributed to the article and approved the submitted version.

Funding

This project was supported in part by grants from the National Key R&D Program of China (2020YFA0509200), and the National Natural Science Foundation of China (81830081, 31970718, 81972203).

Conflict of interest

The authors declare that the research was conducted in the absence of any commercial or financial relationships that could be construed as a potential conflict of interest.

Publisher's note

All claims expressed in this article are solely those of the authors and do not necessarily represent those of their affiliated organizations, or those of the publisher, the editors and the reviewers. Any product that may be evaluated in this article, or claim that may be made by its manufacturer, is not guaranteed or endorsed by the publisher.

Supplementary material

The Supplementary Material for this article can be found online at: <https://www.frontiersin.org/articles/10.3389/fimmu.2022.1018334/full#supplementary-material>

References

- Sung H, Ferlay J, Siegel RL, Laversanne M, Soerjomataram I, Jemal A, et al. Global cancer statistics 2020: GLOBOCAN estimates of incidence and mortality worldwide for 36 cancers in 185 countries. *CA Cancer J Clin* (2021) 71(3):209–49. doi: 10.3322/caac.21660
- Siegel RL, Miller KD, Fuchs HE, Jemal A. Cancer statistics, 2021. *CA Cancer J Clin* (2021) 71(1):7–33. doi: 10.3322/caac.21654
- Guinney J, Dienstmann R, Wang X, de Reynies A, Schlicker A, Song S, et al. The consensus molecular subtypes of colorectal cancer. *Nat Med* (2015) 21(11):1350–6. doi: 10.1038/nm.3967
- Yue Q, Zhang Y, Wang F, Cao F, Duan X, Bai J, et al. Classification of colorectal carcinoma subtypes based on ferroptosis-associated molecular markers. *World J Surg Oncol* (2022) 20(1):117. doi: 10.1186/s12957-022-02575-5
- Cho EJ, Kim M, Jo D, Kim J, Oh JH, Chung HC, et al. Immuno-genomic classification of colorectal cancer organoids reveals cancer cells with intrinsic immunogenic properties associated with patient survival. *J Exp Clin Cancer Res* (2021) 40(1):230. doi: 10.1186/s13046-021-02034-1
- Faubert B, Solmonson A, DeBerardinis RJ. Metabolic reprogramming and cancer progression. *Sci (New York NY)* (2020) 368(6487):eaaw5473. doi: 10.1126/science.aaw5473
- Li X, Wenes M, Romero P, Huang SC-C, Fendt S-M, Ho P-C, et al. Navigating metabolic pathways to enhance antitumor immunity and immunotherapy. *Nat Rev Clin Oncol* (2019) 16(7):425–41. doi: 10.1038/s41571-019-0203-7
- Wei Z, Liu X, Cheng C, Yu W, Yi P. Metabolism of amino acids in cancer. *Front Cell Dev Biol* (2020) 8:603837. doi: 10.3389/fcell.2020.603837
- Najumudeen AK, Ceteci F, Fey SK, Hamm G, Steven RT, Hall H, et al. The amino acid transporter SLC7A5 is required for efficient growth of KRAS-mutant colorectal cancer. *Nat Genet* (2021) 53(1):16–26. doi: 10.1038/s41588-020-00753-3
- Wong CC, Xu J, Bian X, Wu J-L, Kang W, Qian Y, et al. In colorectal cancer cells with mutant KRAS, SLC25A22-mediated glutaminolysis reduces DNA demethylation to increase WNT signaling, stemness, and drug resistance. *Gastroenterology* (2020) 159(6):2163–2180.e6.29. doi: 10.1053/j.gastro.2020.08.016
- Venkateswaran N, Lafita-Navarro MC, Hao Y-H, Kilgore JA, Perez-Castro L, Braverman J, et al. MYC promotes tryptophan uptake and metabolism by the kynurenine pathway in colon cancer. *Genes Dev* (2019) 33(17-18):1236–51. doi: 10.1101/gad.327056.119
- Wu J, Yeung S-CJ, Liu S, Qdaisat A, Jiang D, Liu W, et al. Cyst(e)ine in nutrition formulation promotes colon cancer growth and chemoresistance by activating mTORC1 and scavenging ROS. *Signal Transduct Target Ther* (2021) 6(1):188. doi: 10.1038/s41392-021-00581-9
- Montrose DC, Saha S, Foronda M, McNally EM, Chen J, Zhou XK, et al. Exogenous and endogenous sources of serine contribute to colon cancer metabolism, growth, and resistance to 5-fluorouracil. *Cancer Res* (2021) 81(9):2275–88. doi: 10.1158/0008-5472.CAN-20-1541
- Zhang M, Wang H-Z, Peng R-Y, Xu F, Wang F, Zhao Q, et al. Metabolism-associated molecular classification of colorectal cancer. *Front Oncol* (2020) 10:602498. doi: 10.3389/fonc.2020.602498
- Jiang C, Liu Y, Wen S, Xu C, Gu L. *In silico* development and clinical validation of novel 8 gene signature based on lipid metabolism related genes in colon adenocarcinoma. *Pharmacol Res* (2021) 169:105644. doi: 10.1016/j.phrs.2021.105644
- Zuo D, Li C, Liu T, Yue M, Zhang J, Ning G, et al. Construction and validation of a metabolic risk model predicting prognosis of colon cancer. *Sci Rep* (2021) 11(1):6837. doi: 10.1038/s41598-021-86286-z
- Wang H, Rong X, Zhao G, Zhou Y, Xiao Y, Ma D, et al. The microbial metabolite trimethylamine n-oxide promotes antitumor immunity in triple-negative breast cancer. *Cell Metab* (2022) 34(4):581–94 e8. doi: 10.1016/j.cmet.2022.02.010
- Possemato R, Marks KM, Shaul YD, Pacold ME, Kim D, Birsoy K, et al. Functional genomics reveal that the serine synthesis pathway is essential in breast cancer. *Nature* (2011) 476(7360):346–50. doi: 10.1038/nature10350
- Xu T, Le TD, Liu L, Su N, Wang R, Sun B, et al. CancerSubtypes: an R/Bioconductor package for molecular cancer subtype identification, validation and visualization. *Bioinformatics* (2017) 33(19):3131–3. doi: 10.1093/bioinformatics/btx378
- Mayakonda A, Lin D-C, Assenov Y, Plass C, Koeffler HP. Maftools: efficient and comprehensive analysis of somatic variants in cancer. *Genome Res* (2018) 28(11):1747–56. doi: 10.1101/gr.239244.118
- Eide PW, Bruun J, Lothe RA, Sveen A. CMScaller: An R package for consensus molecular subtyping of colorectal cancer pre-clinical models. *Sci Rep* (2017) 7(1):16618. doi: 10.1038/s41598-017-16747-x
- Ritchie ME, Phipson B, Wu D, Hu Y, Law CW, Shi W, et al. Limma powers differential expression analyses for RNA-sequencing and microarray studies. *Nucleic Acids Res* (2015) 43(7):e47. doi: 10.1093/nar/gkv007
- Yu G, Wang L-G, Han Y, He Q-Y. clusterProfiler: An R package for comparing biological themes among gene clusters. *OMICS* (2012) 16(5):284–7. doi: 10.1089/omi.2011.0118
- Yu G, He Q-Y. ReactomePA: an R/Bioconductor package for reactome pathway analysis and visualization. *Mol Biosyst* (2016) 12(2):477–9. doi: 10.1039/C5MB00663E
- Hanzelmann S, Castelo R, Guinney J. GSVA: Gene set variation analysis for microarray and RNA-seq data. *BMC Bioinf* (2013) 14:7. doi: 10.1186/1471-2105-14-7
- Rosario SR, Long MD, Affronti HC, Rowsam AM, Eng KH, Smiraglia DJ, et al. Pan-cancer analysis of transcriptional metabolic dysregulation using the cancer genome atlas. *Nat Commun* (2018) 9(1):5330. doi: 10.1038/s41467-018-07232-8
- Shukla SA, Bachireddy P, Schilling B, Galonska C, Zhan Q, Bango C, et al. Cancer-germline antigen expression discriminates clinical outcome to CTLA-4 blockade. *Cell* (2018) 173(3):624–33.e8. doi: 10.1016/j.cell.2018.03.026
- Ayers M, Lunceford J, Nebozhyn M, Murphy E, Loboda A, Kaufman DR, et al. IFN- γ -related mRNA profile predicts clinical response to PD-1 blockade. *J Clin Invest* (2017) 127(8):2930–40. doi: 10.1172/JCI91190
- Hu F-F, Liu C-J, Liu L-L, Zhang Q, Guo A-Y. Expression profile of immune checkpoint genes and their roles in predicting immunotherapy response. *Brief Bioinform* (2021) 22(3):bbaa176. doi: 10.1093/bib/bbaa176
- Givechian KB, Wnuk K, Garner C, Benz S, Garban H, Rabizadeh S, et al. Identification of an immune gene expression signature associated with favorable clinical features in treg-enriched patient tumor samples. *NPJ Genom Med* (2018) 3:14. doi: 10.1038/s41525-018-0054-7
- Schütte M, Risch T, Abdavi-Azar N, Boehnke K, Schumacher D, Keil M, et al. Molecular dissection of colorectal cancer in pre-clinical models identifies biomarkers predicting sensitivity to EGFR inhibitors. *Nat Commun* (2017) 8:14262. doi: 10.1038/ncomms14262
- Newman AM, Steen CB, Liu CL, Gentles AJ, Chaudhuri AA, Scherer F, et al. Determining cell type abundance and expression from bulk tissues with digital cytometry. *Nat Biotechnol* (2019) 37(7):773–82. doi: 10.1038/s41587-019-0114-2
- Becht E, Giraldo NA, Lacroix L, Buttard B, Elarouci N, Petitprez F, et al. Estimating the population abundance of tissue-infiltrating immune and stromal cell populations using gene expression. *Genome Biol* (2016) 17(1):218. doi: 10.1186/s13059-016-1070-5
- Yoshihara K, Shahmoradgol M, Martínez E, Vegesna R, Kim H, Torres-García W, et al. Inferring tumour purity and stromal and immune cell admixture from expression data. *Nat Commun* (2013) 4:2612. doi: 10.1038/ncomms3612
- Andri Signorell et mult. al. DescTools: Tools for descriptive statistics (2022). Available at: <https://cran.r-project.org/package=DescTools>.
- Maeser D, Gruener RF, Huang RS. oncoPredict: an R package for predicting *in vivo* or cancer patient drug response and biomarkers from cell line screening data. *Brief Bioinform* (2021) 22(6):bbab260. doi: 10.1093/bib/bbab260
- Yang W, Soares J, Greninger P, Edelman EJ, Lightfoot H, Forbes S, et al. Genomics of drug sensitivity in cancer (GDSC): a resource for therapeutic biomarker discovery in cancer cells. *Nucleic Acids Res* (2013) 41:D955–61. doi: 10.1093/nar/gks1111
- Roh W, Chen P-L, Reuben A, Spencer CN, Prieto PA, Miller JP, et al. Integrated molecular analysis of tumor biopsies on sequential CTLA-4 and PD-1 blockade reveals markers of response and resistance. *Sci Transl Med* (2017) 9(379):eaah3560. doi: 10.1126/scitranslmed.aah3560
- Wu Y, Yang S, Ma J, Chen Z, Song G, Rao D, et al. Spatiotemporal immune landscape of colorectal cancer liver metastasis at single-cell level. *Cancer Discov* (2022) 12(1):134–53. doi: 10.1158/2159-8290.CD-21-0316
- Cancer Genome Atlas N Comprehensive molecular characterization of human colon and rectal cancer. *Nature* (2012) 487(7407):330–7. doi: 10.1038/nature11252
- Samowitz WS, Sweeney C, Herrick J, Albertsen H, Levin TR, Murtaugh MA, et al. Poor survival associated with the BRAF V600E mutation in microsatellite-stable colon cancers. *Cancer Res* (2005) 65(14):6063–9. doi: 10.1158/0008-5472.CAN-05-0404

42. Rowan A, Halford S, Gaasenbeek M, Kemp Z, Sieber O, Volikos E, et al. Refining molecular analysis in the pathways of colorectal carcinogenesis. *Clin Gastroenterol Hepatol* (2005) 3(11):1115–23. doi: 10.1016/S1542-3565(05)00618-X
43. Ceccarelli C, Piazzi G, Paterini P, Pantaleo MA, Taffurelli M, Santini D, et al. Concurrent EGFR and cox-2 expression in colorectal cancer: proliferation impact and tumour spreading. *Ann Oncol: Off J Eur Soc For Med Oncol* (2005) 16(Suppl 4):iv74–iv9. doi: 10.1093/annonc/mdi912
44. Benvenuti S, Sartore-Bianchi A, Di Nicolantonio F, Zanon C, Moroni M, Veronese S, et al. Oncogenic activation of the RAS/RAF signaling pathway impairs the response of metastatic colorectal cancers to anti-epidermal growth factor receptor antibody therapies. *Cancer Res* (2007) 67(6):2643–8. doi: 10.1158/0008-5472.CAN-06-4158
45. Stintzing S, Tejpar S, Gibbs P, Thiebach L, Lenz H-J. Understanding the role of primary tumour localisation in colorectal cancer treatment and outcomes. *Eur J Cancer* (2017) 84:69–80. doi: 10.1016/j.ejca.2017.07.016
46. Leach JDG, Vlahov N, Tsantoulis P, Ridgway RA, Flanagan DJ, Gilroy K, et al. Oncogenic BRAF, unrestrained by TGF β -receptor signalling, drives right-sided colonic tumorigenesis. *Nat Commun* (2021) 12(1):3464. doi: 10.1038/s41467-021-23717-5
47. Rustgi AK. BRAF: a driver of the serrated pathway in colon cancer. *Cancer Cell* (2013) 24(1):1–2. doi: 10.1016/j.ccr.2013.06.008
48. Hanahan D. Hallmarks of cancer: New dimensions. *Cancer Discov* (2022) 12(1):31–46. doi: 10.1158/2159-8290.CD-21-1059
49. Wasserman I, Lee LH, Ogino S, Marco MR, Wu C, Chen X, et al. SMAD4 loss in colorectal cancer patients correlates with recurrence, loss of immune infiltrate, and chemoresistance. *Clin Cancer Res* (2019) 25(6):1948–56. doi: 10.1158/1078-0432.CCR-18-1726
50. Jia Q, Wang J, He N, He J, Zhu B. Titin mutation associated with responsiveness to checkpoint blockades in solid tumors. *JCI Insight* (2019) 4(10):e127901. doi: 10.1172/jci.insight.127901
51. Li P, Xiao J, Zhou B, Wei J, Luo J, Chen W, et al. SYNE1 mutation may enhance the response to immune checkpoint blockade therapy in clear cell renal cell carcinoma patients. *Aging* (2020) 12(19):19316–24. doi: 10.18632/aging.103781
52. Li X, Pasche B, Zhang W, Chen K. Association of MUC16 mutation with tumor mutation load and outcomes in patients with gastric cancer. *JAMA Oncol* (2018) 4(12):1691–8. doi: 10.1001/jamaoncol.2018.2805
53. Zhang L, Han X, Shi Y. Association of MUC16 mutation with response to immune checkpoint inhibitors in solid tumors. *JAMA Netw Open* (2020) 3(8):e2013201. doi: 10.1001/jamanetworkopen.2020.13201
54. Guardia T, Eason M, Kontogianni-Konstantopoulos A. Obscurin: A multitasking giant in the fight against cancer. *Biochim Biophys Acta (BBA) - Rev Cancer* (2021) 1876(1):188567. doi: 10.1016/j.bbcan.2021.188567
55. Tuntithavornwat S, Shea DJ, Wong BS, Guardia T, Lee SJ, Yankaskas CL, et al. Giant obscurin regulates migration and metastasis via RhoA-dependent cytoskeletal remodeling in pancreatic cancer. *Cancer Lett* (2022) 526:155–67. doi: 10.1016/j.canlet.2021.11.016
56. Yu J, Wu WKK, Li X, He J, Li X-X, Ng SSM, et al. Novel recurrently mutated genes and a prognostic mutation signature in colorectal cancer. *Gut* (2015) 64(4):636–45. doi: 10.1136/gutjnl-2013-306620
57. Counihan JL, Grossman EA, Nomura DK. Cancer metabolism: Current understanding and therapies. *Chem Rev* (2018) 118(14):6893–923. doi: 10.1021/acs.chemrev.7b00775
58. Du T, Han J. Arginine metabolism and its potential in treatment of colorectal cancer. *Front Cell Dev Biol* (2021) 9:658861. doi: 10.3389/fcell.2021.658861
59. Badeaux MD, Rolig AS, Agnello G, Enzler D, Kasiewicz MJ, Priddy L, et al. Arginase therapy combines effectively with immune checkpoint blockade or agonist anti-OX40 immunotherapy to control tumor growth. *Cancer Immunol Res* (2021) 9(4):415–29. doi: 10.1158/2326-6066.CIR-20-0317
60. Geeraerts SL, Heylen E, De Keersmaecker K, Kampen KR. The ins and outs of serine and glycine metabolism in cancer. *Nat Metab* (2021) 3(2):131–41. doi: 10.1038/s42255-020-00329-9
61. Hattori A, Tsunoda M, Konuma T, Kobayashi M, Nagy T, Glushka J, et al. Cancer progression by reprogrammed BCAA metabolism in myeloid leukaemia. *Nature* (2017) 545(7655):500–4. doi: 10.1038/nature22314
62. Raffel S, Falcone M, Kneisel N, Hansson J, Wang W, Lutz C, et al. BCAT1 restricts α KG levels in AML stem cells leading to IDHmut-like DNA hypermethylation. *Nature* (2017) 551(7680):384–8. doi: 10.1038/nature24294
63. Li J-T, Yin M, Wang D, Wang J, Lei M-Z, Zhang Y, et al. BCAT2-mediated BCAA catabolism is critical for development of pancreatic ductal adenocarcinoma. *Nat Cell Biol* (2020) 22(2):167–74. doi: 10.1038/s41556-019-0455-6
64. Ikeda K, Kinoshita M, Kayama H, Nagamori S, Kongpracha P, Umemoto E, et al. Slc3a2 mediates branched-chain amino-Acid-Dependent maintenance of regulatory T cells. *Cell Rep* (2017) 21(7):1824–38. doi: 10.1016/j.celrep.2017.10.082
65. Silva LS, Poschet G, Nonnenmacher Y, Becker HM, Sapcariu S, Gaupel A-C, et al. Branched-chain ketoacids secreted by glioblastoma cells via MCT1 modulate macrophage phenotype. *EMBO Rep* (2017) 18(12):2172–85. doi: 10.15252/embr.201744154
66. Ananieva EA, Patel CH, Drake CH, Powell JD, Hutson SM. Cytosolic branched chain aminotransferase (BCATc) regulates mTORC1 signaling and glycolytic metabolism in CD4+ T cells. *J Biol Chem* (2014) 289(27):18793–804. doi: 10.1074/jbc.M114.554113
67. Peng H, Wang Y, Luo W. Multifaceted role of branched-chain amino acid metabolism in cancer. *Oncogene* (2020) 39(44):6747–56. doi: 10.1038/s41388-020-01480-z
68. Aimi F, Moch H, Schraml P, Hottiger MO. Cytoplasmic ADP-ribosylation levels correlate with markers of patient outcome in distinct human cancers. *Modern Pathol* (2021) 34(8):1468–77. doi: 10.1038/s41379-021-00788-9
69. Caon I, Bartolini B, Parnigoni A, Caravà E, Moretto P, Viola M, et al. Revisiting the hallmarks of cancer: The role of hyaluronan. *Semin Cancer Biol* (2020) 62:9–19. doi: 10.1016/j.semcancer.2019.07.007
70. Wang D, DuBois RN. Role of prostanoids in gastrointestinal cancer. *J Clin Invest*. 2018 128(7):2732–42. doi: 10.1172/JCI97953